International Journal of Earth Sciences Knowledge and Applications
journal homepage: http://www.ijeska.com/index.php/ijeska

Research Article

e-ISSN: 2687-5993

Vegetation Distribution Pattern at Several Landforms and Its Implications towards Surface Run Off

Fahmi Arif Kurnianto[1]*, Elan Artono Nurdin[1], Era Iswara Pangastuti[1], Hani Dwi Ribtyanti[1]

[1]*Geography Education Study Program, University of Jember, East Java, 68121, Indonesia*

INFORMATION

Article history
Received 07 July 2023
Revised 02 August 2023
Accepted 02 August 2023

Keywords
Vegetation distribution
Landform
Run off
Land use
Regional planning

Contact
*Fahmi Arif Kurnianto
fahmiarif.fkip@unej.ac.id

ABSTRACT

Mapping of vegetation and other land cover is very important for monitoring the development of land use change and regional planning. However, mapping that focuses on differences in landform characteristics is still very limited. This study aims to analyze the pattern of vegetation distribution in karst, volcanic, and fold landforms. NDVI was used to analyze the distribution of vegetation in several landforms, while MODIS data was used to analyze the intensity and fluctuation of run off in the study area. This study used Sentinel 2 imagery as a data source with a spatial resolution of 10 meters and a temporal resolution of 16-30 days. The results show that there is a different pattern of vegetation distribution in conical hills (holokarst), quaternary volcanic hills, and fold hills. In karst landforms, vegetation is spread out following the distribution of conical hills. In the folded hills, the vegetation is spread in the direction of the anticline axis distribution, while the vegetation is evenly distributed in the volcanic hills with high vegetation density. Differences in the distribution of vegetation also have an impact on differences in surface run off for the three landforms. The distribution of vegetation in several landforms can efficiently be identified using the vegetation index and sentinel 2 because of the wider area coverage, so that it can affect regional environmental management.

1. Introduction

Increased human activities lead to the potential for landscape degradation (Tarolli and Sofia, 2016). Research using the Digital Elevation Model (DEM) in geomorphology has been carried out by several previous researchers. The results of the research of O'Loughlin et al. (2016) show that the use of DEM by reducing the error rate can be used to detect vegetation patterns and their relationship to flood modeling. Boulton and Stokes (2018) found that DEM with a resolution of 12 m can analyze drainage networks and regional geomorphological analysis. Meanwhile, Garosi et al. (2018) found that the optimal pixel is 10 m for several algorithm models used to identify gully erosion.

Digital Soil Mapping can analyze the physical and chemical characteristics of the soil with good accuracy (Mosleh et al., 2016). Remote sensing and GIS are effective tools for analyzing morphometry, basin drainage, and geological structures by taking into account the indicators of sediment yield, landmass, and elevations (Kaliraj et al., 2015; Zwaan et al., 2020; Inzana et al., 2003). Remote sensing using Google Earth can analyze the characteristics of several landforms such as coastal and glacial including the erosion process (Boardman, 2016). LULC analysis needs to consider aspects related to vegetation such as evapotranspiration, groundwater, and surface runoff (Setyorini et al., 2017).

OBIA with a spatial resolution of 30 m can help improve the quality of land use management (Alqurashi et al., 2016). The integration of OBIA with Markov chain (MC) and Cellular Automata (CA) modeling results in a better understanding of past, present, and future land cover changes (Gilani et al., 2015; Guan et al., 2011; Naboureh et al., 2017). OBIA is better than per pixel classifiers in analyzing urban land cover (Myint et al., 2011).

Several studies related to landscape evolution in Indonesia have been carried out with a focus on lithology. Some of the

results of these studies include sedimentary basins related to diapirs formed during the Cambrian period influenced by the presence of folds and the shallow marine depositional environment (Hearon et al., 2015). The diapir in East Java is evidenced by a mud volcano (Lumpur Sidoarjo/Lusi) with a characteristic depth of methane 1800 m - 3200 m (Collignon et al., 2018). Kendeng Mountains in Java Island have low velocity with surface geological features (Zulfakriza et al., 2014).

The Northeast Java Basin was formed by a deposition process in a shallow marine environment indicated by foraminifera-rich mudstones (Berghuis et al., 2019). The Northeast Java Basin was formed by various lithologies influenced by faults and subsurface volcanic activity (Nurhandoko et al., 2019). East Java is part of Sundaland with the same character as Borneo (Kalimantan) Island as a result of continental drifting (Metcalfe, 2017). The mud volcano in East Java (Lusi) is also affected by strike-slip faulting, fault escarpment, river deviation and railroad as evidence of the existence of the Watukosek fault system (Obermann et al., 2018).

Previous studies related to the relationship between vegetation distribution and landscapes have been carried out by several researchers. The results of these studies include: hydrogeo-geomorphological aspects are indicators in seeing differences in vegetation distribution (Urgeghe et al., 2021). Vegetation mapping with high spatial resolution and increasing temporal resolution every month is able to detect fluvial land changes (Pu et al., 2021). The Disaster Vegetation Damage Index has an association with crop yield loss by considering the flood inundation extents parameter (Rahman et al., 2021). Spatial distribution of plants on floodplains is influenced by flood stress by considering water level parameters (Martinez and le Toan, 2007). Time-series of multiple indices can improve analysis of flood dynamics by utilizing daily MODIS (Mohammadi et al., 2017).

Vegetation composition can be predicted with high accuracy by utilizing the multi-season Sentinel-2 imagery (Macintyre et al., 2020). Vegetation distribution is influenced by elevation by considering soil water index and elevation factors (Casalini et al., 2019; Gregory et al., 2019; Larsen, 2019). Decreasing of vegetation density at the watershed has been detected by using Landsat 8 with NDVI (Putera et al., 2019). ASTER Imagery data has detected tree canopy cover by using MSAVI (Anurogo et al., 2018).

A few researchers focused on the relationship between landforms and vegetation distribution patterns. There have been limited studies concerned with the comparison of 3 landforms by considering the aspect of the vegetation distribution pattern. Therefore, this research intends to compare the pattern of vegetation distribution on volcanic landforms, folds landform, and karst landform in tropical regions. This comparison is very important due to folded landforms with interspersed rock lithology, tertiary sedimentary rocks have flood susceptibility, particularly in tropical areas. Therefore, this study aims to map the pattern and distribution of vegetation based on the characteristics of the landforms.

2. Methods

2.1. Study Area

This study is located in the eastern part of Java Island by taking 3 samples of the area purposively with consideration of differences in morphography and morphogenesis of landforms. The sample area taken consisted of folded hills, conical hills on holokarst landscapes, and volcanic hills.

2.2. Image Processing

This study used sentinel 2 imagery with a spatial resolution of 10 meters, 12-bit radiometric resolution, and a temporal resolution of 15-30 days. Data recording time starts from February 2021 to April 2022. Atmospheric correction is used to get better recording results (Nazeer et al., 2014). Google Earth Engine is used to process sentinel 2 imagery which includes filtering with minimum cloud cover, mosaic, composite, image enhancement and clipping. This study uses channels 2, 3, 4, 5, 6, 7, 8, 8A, 11 and 12 (Blue, Green, Red, Red Edge 1 - 4, NIR, SWIR – 2). This study also used sentinel 1 to determine the morphology.

2.3. Data Analysis

To analyze the vegetation density, sentinel 2 imagery with the NDVI method was used. Areas with dense vegetation will be indicated in light green, while areas with low vegetation density will be indicated in lighter colors. A low NDVI value indicates vegetation with moisture stress and a higher value indicates a higher vegetation density. This identification is also used for drought early warning (Wardlow and Egbert, 2010). Furthermore, MODIS satellite data is used to analyze the runoff and precipitation distribution. The analyzed areas include folded hilly landscapes, karst landscapes, and volcanic landscapes in eastern Java.

3. Results and Discussion

The vegetation index in East Java shows the difference between the north coast and the south coast (Fig. 1A). The North coast has a brighter color which indicates a low density of vegetation, whereas the central and southern areas have a clearer green color because they have denser vegetation. On the North coast, the sediment supply is partly derived from shallow marine deposition as indicated by the presence of tertiary sedimentary rock stratigraphy, while in the central and southern regions the basic relief stratigraphy is strongly influenced by volcanic landscapes.

Fig. 1B shows the existence of different vegetation distribution patterns based on the vegetation index; in the hills the vegetation folds spread following the anticline direction. In volcanic landforms, the vegetation is very dense, which also indicates the presence of well-developed and evenly distributed volcanic soil (Fig. 1D). In the conical karst hills landscape, it is seen that the distribution of vegetation follows the distribution of conical karst hills (Fig. 1C).

Whereas in karst valleys the vegetation density is lower because in this area there are many sinkholes which are places for underground river recharge. In this valley area, there is also a lot of surface runoff that cannot be absorbed optimally because the dominant soil in this area is Mediterranean soil resulting from weathering of limestone.

Fig. 3A shows that the folded hilly landforms have a fairly high runoff due to the characteristics of the soil which is the result of pedogenesis from bedrock. Meanwhile, the karst landscape has the lowest run-off due to the large number of sinkholes and underground rivers (Fig. 3B). Regions with volcanic landforms have the highest runoff due to higher rainfall (Fig. 3C).

The comparison between holokarst hills (Fig. 4A), folded hills (Fig. 4B), and volcanic hills (Fig. 4C) shows that there is a pattern of vegetation distribution based on landform. The distribution and pattern of vegetation in the holokarst follows the karst cone (Fig. 4A). The soil profile of the holokarst is not thick with low surface water supply, causing no vegetation to be found in the valleys around the karst cone. Surface water in the holokarst landform is very low due to the presence of sinkholes that change the direction of the surface river flow into an underground river. In holokarst hills, the soil is formed by weathering of carbonate rocks that are below the surface. Holokarst formed in the fore-arc basin with high tectonic intensity, thus forming many sinkholes and extensive underground river systems (Fig. 4A). With thin soil, this area is unable to produce sufficient organic matter and nutrients for plants, resulting in uneven distribution of vegetation. In the fore-arc region with high tectonic intensity, a transgressive facies system is found with the stratigraphic sequence of carbonate rock is very dominant at the top and then followed by volcanic rock.

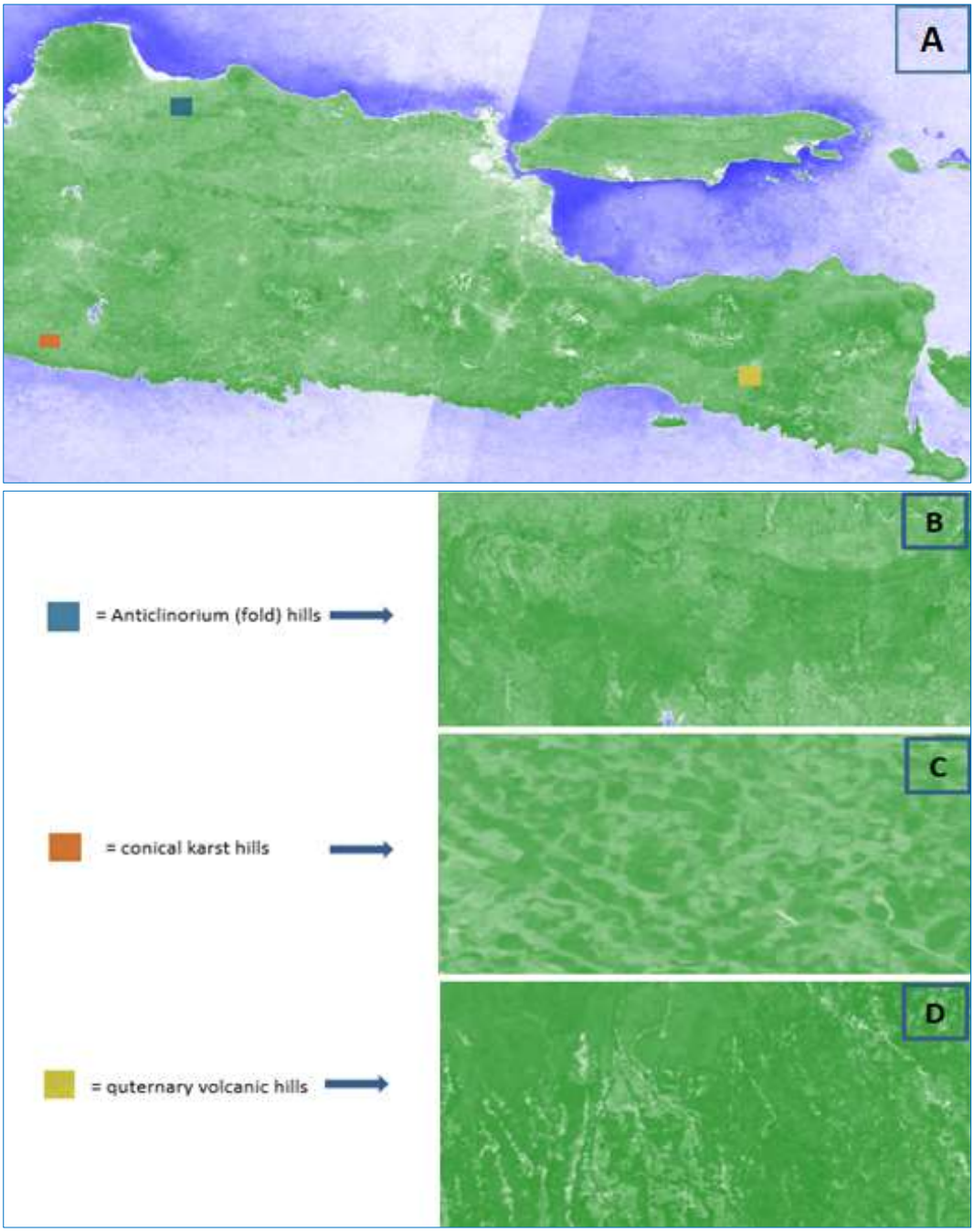

Fig. 1. (A) Vegetation density of East Java, (B) Vegetation density and pattern of fold hills, (C) Vegetation density and pattern of conical (holokarst) hills and (D) Vegetation density of quaternary volcanic hills

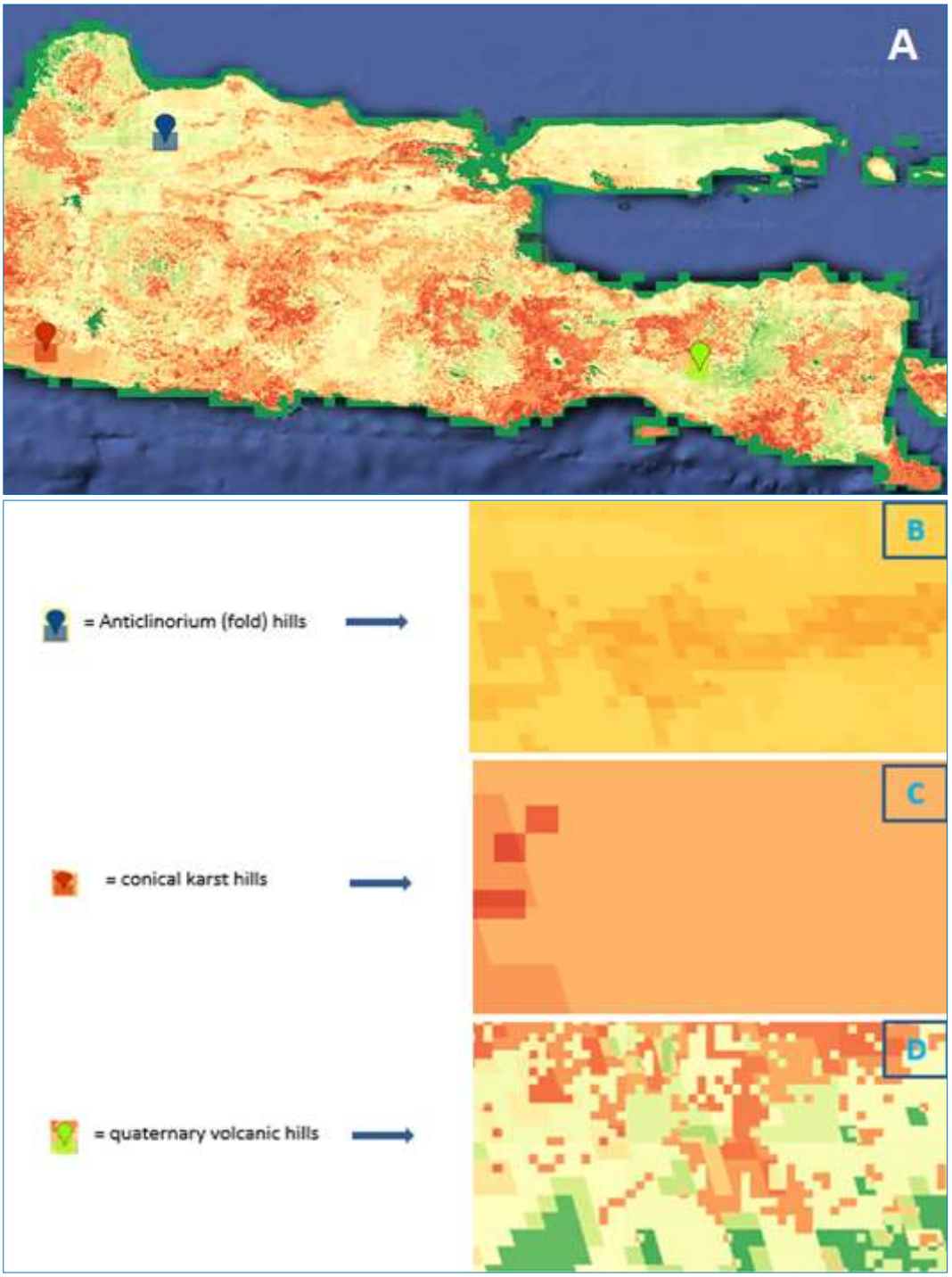

Fig. 2. (A) Run off distribution of East Java, (B) Run off distribution of fold hills, (C) Run off distribution of conical (holokarst) hills and (D) Run off distribution of quaternary volcanic hills

In the folded hills (Fig. 5), it can be seen that the distribution of vegetation follows the direction of the longitudinal and circular folds. Circular hills show a plunging anticline formed by a combination of tertiary sedimentary rock lithology (Fig. 5b).

On the lower hillside, less vegetation can be seen due to the different types of tertiary sedimentary rocks. The influence of volcanism on the folded hills is very low due to its location in the back-arc basin with a radius far from subduction and quarter arc volcanoes (Fig. 5).

This alternation of tertiary sedimentary rocks is different from that which occurs with lithology in front of the arc. In the anticline hills, carbonate rocks are not dominant because they are interspersed with other tertiary sedimentary rocks. The characteristics of the alternation are following an anticlinorium pattern with the character of old rocks being exposed on the surface due to the influence of anticline.

In addition, the interstitial age of tertiary sedimentary rocks is included in the age that produces soil types with low quality. Field findings also show that in this area there are

many fossils from shallow seas in the tertiary period which indicate this anticline hill area is a shallow sea behind the arc with low tectonic intensity.

Fig. 6 shows that the distribution of vegetation on the volcanic hills is very flat and can be found in all parts of the hills. This is because the volcanic hills area is composed of quaternary volcanic rock lithology which has the ability to form volcanic soil with very thick characteristics and has high organic matter (Fig. 6c). The closer distance to subduction causes eruptions to still occur and also affects the intensity of soil rejuvenation in all parts of the quarter volcanic hills.

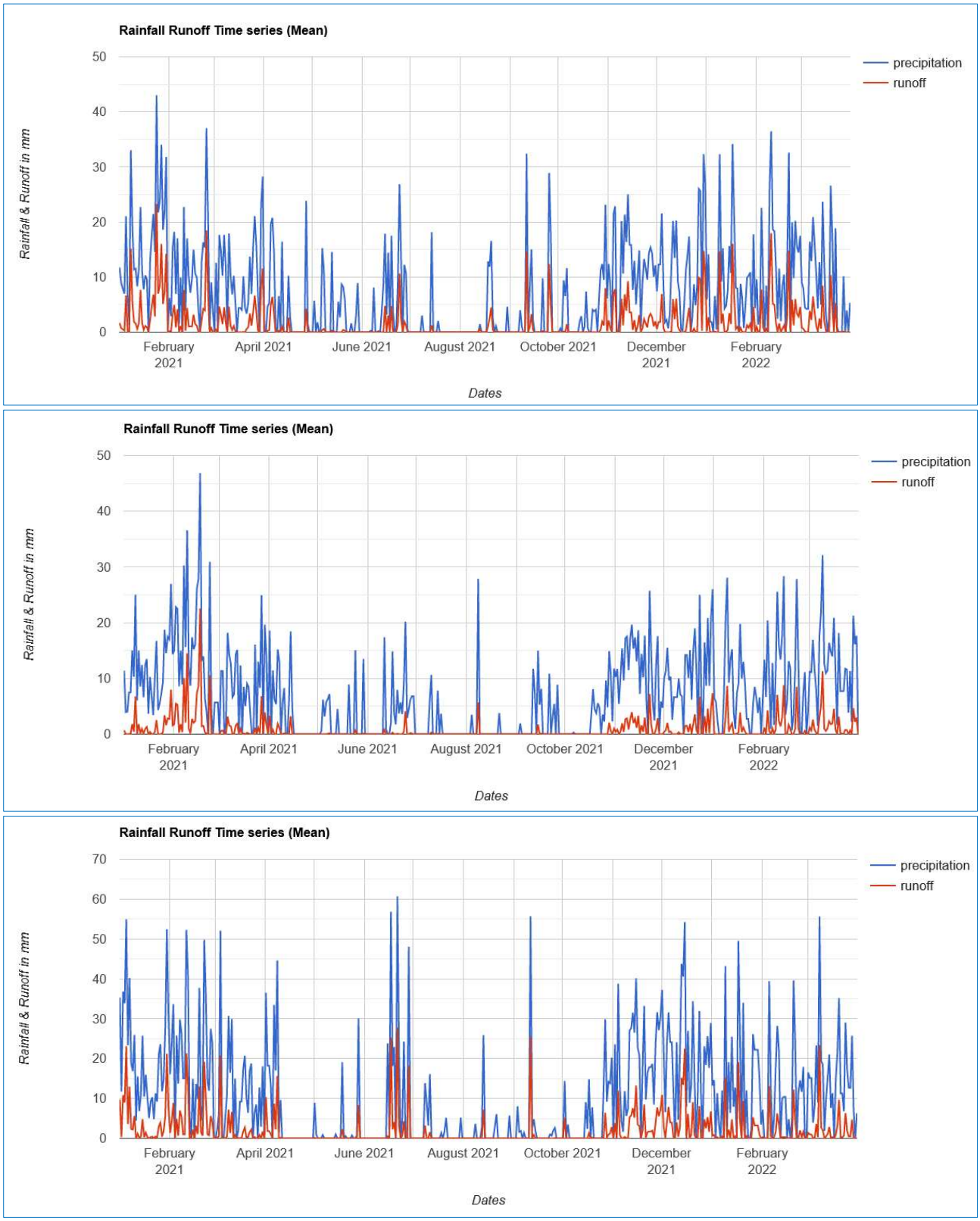

Fig. 3. (A) Run off and rainfall of fold hills, (B) Run off and rainfall of conical (holokarst) hills and (C) Run off distribustion of quaternary volcanic hills

Fig. 4. A) holokarst hills, B) folded hills and C) volcanic hills by google earth

Low vegetation density is related to the tectonic evolution of coastal areas. In areas with tertiary sedimentary rock lithology with transgressive facies type, a relationship has been found between the presence of a very wide limestone lithology interspersed with sandstone and silt of tertiary age. This combination causes the low ability of the soil in the infiltration process in the fold hills behind the arc. The soil that is formed does not have a texture balance, mainly due to the presence of carbonate rocks which have very low infiltration capabilities. In the folded hilly area with carbonate rocks with a mesokarst system, the secondary porosity is not formed perfectly.

Fig. 5. A) topography map of fold hills, B) fold hills by Sentinel-1 and C) fold hills by google earth

Fig. 6. A) topography map of volcanic hills, B) volcanic hills by Sentinel-1 and C) volcanic hills by google earth

This is different when compared to carbonated rocks in front of the arc which develop secondary porosity (allogenic and autogenic system). In the coastal areas of northern Java, eastern Sumatra, the coast in Kalimantan will have deposition formed by sediments (sandstone, siltstone, claystone). This has an impact on the ease with which the beach is eroded with a shoreline that is easy to shift. This will certainly disrupt the ecosystem around the coast which is very rich in various kinds of biota.

The sedimentary rock is a representation of the high intensity of deposition which generally takes place starting in the tertiary period. The north coast of East Java (Folds Region) is one clear example of sediment accumulation in the tertiary

era (Figs. 7a and 7e). The composite image of Sentinel-2 (Fig. 7) shows a significant difference between volcanic landforms and folds. In the fold's landform, run off and intensive delta formation are found. This is evidenced by the number of watersheds in the northern part of East Java which are influenced by the folding process.

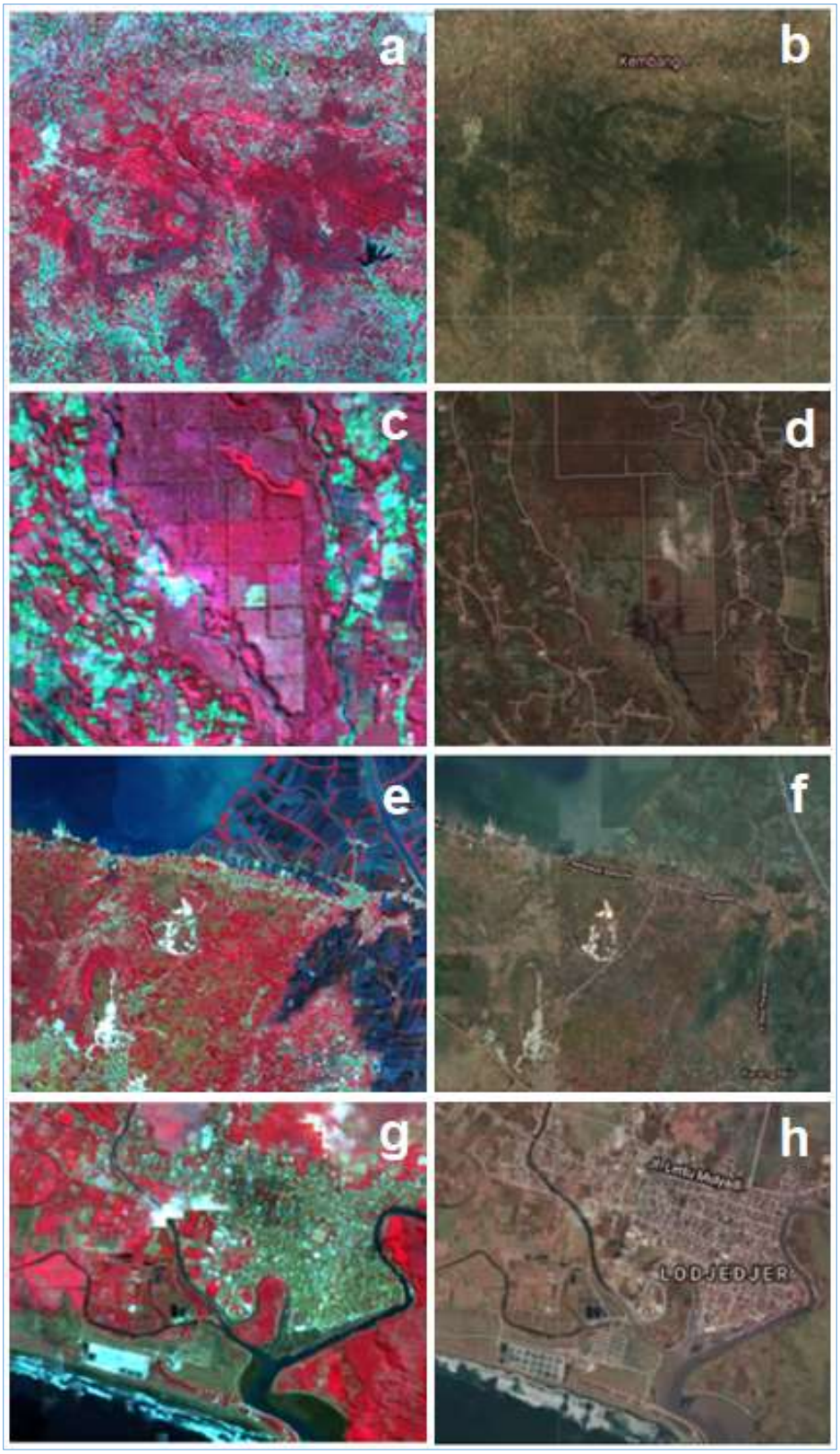

Fig. 7. a) Fold hills by Sentinel-2 Composite, b) Fold hills by google earth, c) Volcanic hills by Sentinel-2 Composite, d) Volcanic hills by Google earth, e) Alluvial at back arc basin by Sentinel-2 Composite, f) d) Alluvial at back arc basin by Google earth, g) Alluvial at front arc basin by Sentinel-2 Composite and h) Alluvial at front arc basin by Google Earth

On the other hand, the south coast of East Java is evidence of a very intensive fault given the proximity to the subduction zone. This causes a steep coastal landscape with many cliffs and has a narrower river morphometry than the river in the north, as a result of which less sediment material is carried to the coast than on the north coast of Java. The northern coast of Java and eastern Kalimantan produce large deltaic landforms, while the southern coast of Java is very rare to find large deltas. The sediment that has accumulated on the northern coast of Java is much larger because it is carried by rivers with wide channels that pass-through rocks that are not resistant to erosion.

In the watershed system, these large rivers will form a lot of meanders and a lot of floodplains given the high lateral erosion. Thus, the material carried to the coast is very large. There is a congruence and strong relationship between vegetation distribution patterns and landform characteristics. This can reduce bias in sampling and test accuracy in remote sensing image processing. Weaknesses in the image accuracy test in analyzing land in previous studies only considered pixel values without paying attention to geological conditions and landforms. The results of this study are different from previous studies, among others: A study on land cover using a comparison algorithm has been carried out by Adam et al. (2014) and Ghosh and Joshi (2014) showed similar classification results for SVM and RF.

Other research results by other research results by Khatami et al. (2016) found that SVM, kNN, and RF have better accuracy than other algorithms. Meanwhile Meanwhile, Heydari and Mountrakis (2018) compared 5 classification algorithms and found that SVM and KNN are the best classifications. In the identification of landforms, the algorithm cannot measure tectonic evolution and other characteristics such as associations with lithology, tectonic elements, and land potential in full. Therefore, the results of this study can complement the findings of previous studies, especially in geomorphological and vegetation mapping.

Important findings in our study also relate to the management of natural resources, especially vegetation. Our research findings indicate that areas with low density vegetation patterns are strongly influenced by back-arc tectonic elements. Therefore, a region like this couldn't be utilized in the same way as the arc's front region. Meanwhile, land cover mapping in previous studies only focused on calculating the general area of vegetation which could cause errors in detecting soil thickness and the ability of the soil to respond to water. This error will result in a very high risk of natural disasters.

Some of these previous studies include: The integration of optical and radar sensors using crowdsourced ground truth data has been carried out by (Wang et al., 2020) to identify rice and cotton crops in India, while Slagter et al. (2020) mapped wetlands in South Africa. Orynbaikyzy et al. (2019) found improved plant classification results in northern Germany by combining radar and optical data. The integration of Sentinel-2 with PlanetScope was carried out by Mercier et al. (2019) in Paragominas (Brazil) and Gašparović and Jogun (2018) for mapping and monitoring vegetation with findings that there is an increase in classification results.

4. Conclusion

The distribution pattern of vegetation in several landforms has different characteristics caused by tectonic elements and soil characteristics. The distribution of vegetation in the folded hills follows the direction of the anticline axis with high surface run off due to the pedogenesis of tertiary sedimentary rocks. The distribution of vegetation in the karst landscape follows the distribution of conical hills with low surface run off values due to the development of underground rivers, while volcanic hills have the highest vegetation index values with high run off due to rainfall intensity.

References

Adam, E., Mutanga, O., Odindi, J., Abdel-Rahman, E.M., 2014. Land-use/cover classification in a heterogeneous coastal landscape using RapidEye imagery: evaluating the performance of random forest and support vector machines classifiers. International Journal of Remote Sensing 35 (10), 3440-3458. https://doi.org/10.1029/2018TC005010.

Advokaat, E.L., Marshall, N.T., Li, S., Spakman, W., Krijgsman, W., van Hinsbergen, D.J.J., 2018. Cenozoic rotation history of borneo and sundaland, SE asia revealed by paleomagnetism, seismic tomography, and kinematic reconstruction. Tectonics 37 (8), 2486-2512. https://doi.org/10.1029/2018TC005010.

Alqurashi, A.F., Kumar, L., Sinha, P., 2016. Urban land cover change modelling using time-series satellite images: A case study of urban growth in five cities of Saudi Arabia. Remote Sensing 8 (10), 838. https://doi.org/10.3390/rs8100838.

Anurogo, W., Lubis, M.Z., Mufida, M.A.K., 2018. Modified soil-adjusted vegetation index in multispectral remote sensing data for estimating tree canopy cover density at rubber plantation. Journal of Geoscience, Engineering, Environment, and Technology 3 (1), 15-24.

Berghuis, H.W.K., Troelstra, S.R., Zaim, Y., 2019. Plio-pleistocene foraminiferal biostratigraphy of the eastern kendeng zone (java, indonesia): The marmoyo and sumberingin sections. Palaeogeography, Palaeoclimatology, Palaeoecology 528, 218-231. https://doi.org/10.1016/j.palaeo.2019.05.008.

Boardman, J., 2016. The value of google earth™ for erosion mapping. Catena 143, 123-127. https://doi.org/10.1016/j.catena.2016.03.031.

Boulton, S.J., Stokes, M., 2018. Which DEM is best for analyzing fluvial landscape development in mountainous terrains? Geomorphology 310, 168-187. https://doi.org/10.1016/j.geomorph.2018.03.002.

Casalini, A.I., Bouza, P.J., Bisigato, A.J. 2019. Geomorphology, soil and vegetation patterns in an arid ecotone. Catena 174, 353-361.

Collignon, M., Schmid, D.W., Galerne, C., Lupi, M., Mazzini, A., 2018. Modelling fluid flow in clastic eruptions: Application to the lusi mud eruption. Marine and Petroleum Geology 90, 173-190. https://doi.org/10.1016/j.marpetgeo.2017.08.011.

Corenblit, D., Tabacchi, E., Steiger, J., Gurnell, A.M., 2007. Reciprocal interactions and adjustments between fluvial landforms and vegetation dynamics in river corridors: A review of complementary approaches. Earth-Science Reviews 84 (1-2), 56-86. https://doi.org/10.1016/j.earscirev.2007.05.004.

Endar, B.N.B., Rizal, K., Susilowati, Kaswandhi, T., Sri, W.S., Rizka, A.H.M., Rizal, a.M., Rio, K.M., Elfa, F., Insan, R.K., 2019. Integrated Subsurface Temperature Modeling beneath Mt. Lawu and Mt. Muriah in The Northeast Java Basin,

Indonesia. Open Geosciences 11 (1), 341-351. https://doi.org/10.1515/geo-2019-0027.

Garosi, Y., Sheklabadi, M., Pourghasemi, H.R., Besalatpour, A. A., Conoscenti, C., Van Oost, K., 2018. Comparison of differences in resolution and sources of controlling factors for gully erosion susceptibility mapping. Geoderma 330, 65-78. https://doi.org/10.1016/j.geoderma.2018.05.027.

Gašparović, M., Jogun, T., 2018. The effect of fusing Sentinel-2 bands on land-cover classification. International Journal of Remote Sensing 39 (3), 822-841.

Ghosh, A., Joshi, P.K., 2014. A comparison of selected classification algorithms for mapping bamboo patches in lower Gangetic plains using very high resolution WorldView 2 imagery. International Journal of Applied Earth Observation and Geoinformation 26, 298-311.

Gilani, H., Shrestha, H.L., Murthy, M.S.R., Phuntso, P., Pradhan, S., Bajracharya, B., Shrestha, B., 2015. Decadal land cover change dynamics in bhutan. Journal of Environmental Management 148, 91-100. https://doi.org/10.1016/j.jenvman.2014.02.014.

Gregory, S., Wildman, R., Hulse, D., Ashkenas, L., Boyer, K., 2019. Historical changes in hydrology, geomorphology, and floodplain vegetation of the Willamette River, Oregon. River Research and Applications 35 (8), 1279-1290.

Guan, D., Li, H., Inohae, T., Su, W., Nagaie, T., Hokao, K., 2011. Modeling urban land use change by the integration of cellular automaton and markov model. Ecological Modelling 222 (20-22), 3761-3772. https://doi.org/10.1016/j.ecolmodel.2011.09.009.

Hearon, T.E., Rowan, M.G., Lawton, T.F., Hannah, P.T., Giles, K.A., 2015. Geology and tectonics of neoproterozoic salt diapirs and salt sheets in the eastern willouran ranges, south australia. Basin Research 27 (2), 183-207. https://doi.org/10.1111/bre.12067.

Heydari, S.S., Mountrakis, G., 2018. Effect of classifier selection, reference sample size, reference class distribution and scene heterogeneity in per-pixel classification accuracy using 26 Landsat sites. Remote Sensing of Environment 204, 648-658.

Inzana, J., Kusky, T., Higgs, G., Tucker, R., 2003. Supervised classifications of landsat TM band ratio images and landsat TM band ratio image with radar for geological interpretations of central madagascar. Journal of African Earth Sciences 37 (1-2), 59-72. https://doi.org/10.1016/S0899-5362(03)00071-X.

Kaliraj, S., Chandrasekar, N., Magesh, N.S., 2015. Morphometric analysis of the river thamirabarani sub-basin in kanyakumari district, south west coast of tamil nadu, india, using remote sensing and GIS. Environmental Earth Sciences 73 (11), 7375-7401. https://doi.org/10.1007/s12665-014-3914-1.

Khatami, R., Mountrakis, G., Stehman, S.V., 2016. A meta-analysis of remote sensing research on supervised pixel-based land-cover image classification processes: General guidelines for practitioners and future research. Remote Sensing of Environment 177, 89-100.

Larsen, L.G., 2019. Multiscale flow-vegetation-sediment feedbacks in low-gradient landscapes. Geomorphology 334, 165-193.

Macintyre, P., Van Niekerk, A., Mucina, L., 2020. Efficacy of multi-season Sentinel-2 imagery for compositional vegetation classification. International Journal of Applied Earth Observation and Geoinformation 85, 101980. https://doi.org/10.1016/j.jag.2019.101980.

Martinez, J.M., Le Toan, T., 2007. Mapping of flood dynamics and spatial distribution of vegetation in the Amazon floodplain using multitemporal SAR data. Remote sensing of Environment 108 (3), 209-223.

Mercier, A., Betbeder, J., Rumiano, F., Baudry, J., Gond, V., Blanc, L., Bourgoin, C., Cornu, G., Ciudad, C., Marchamalo, M., Poccard-Chapuis, R. Hubert-Moy, L., 2019. Evaluation of Sentinel-1 and 2-time series for land cover classification of forest–agriculture mosaics in temperate and tropical landscapes. Remote Sensing 11 (8), 979.

Metcalfe, I., 2017. Tectonic evolution of Sundaland. Bulletin of the Geological Society of Malaysia 63, 27-60. https://doi.org/10.7186/bgsm63201702.

Mohammadi, A., Costelloe, J.F., Ryu, D., 2017. Application of time series of remotely sensed normalized difference water, vegetation and moisture indices in characterizing flood dynamics of large-scale arid zone floodplains. Remote sensing of Environment 190, 70-82.

Mosleh, Z., Salehi, M.H., Jafari, A., Borujeni, I.E., Mehnatkesh, A., 2016. The effectiveness of digital soil mapping to predict soil properties over low-relief areas. Environmental Monitoring and Assessment 188 (3), 1-13. https://doi.org/10.1007/s10661-016-5204-8.

Myint, S.W., Gober, P., Brazel, A., Grossman-Clarke, S., Weng, Q., 2011. Per-pixel vs. object-based classification of urban land cover extraction using high spatial resolution imagery. Remote Sensing of Environment 115 (5), 1145-1161. https://doi.org/10.1016/j.rse.2010.12.017.

Naboureh, A., Rezaei Moghaddam, M.H., Feizizadeh, B., Blaschke, T., 2017. An integrated object-based image analysis and CA-markov model approach for modeling land use/land cover trends in the Sarab Plain. Arabian Journal of Geosciences 10 (12). https://doi.org/10.1007/s12517-017-3012-2.

Nazeer, M., Nichol, J.E., Yung, Y.K., 2014. Evaluation of atmospheric correction models and Landsat surface reflectance product in an urban coastal environment. International Journal of Remote Sensing 35 (16), 6271-6291. https://doi.org/10.1080/01431161.2014.951742.

Novak, V., Renema, W., 2018. Ecological tolerances of miocene larger benthic foraminifera from indonesia. Journal of Asian Earth Sciences 151, 301-323. https://doi.org/10.1016/j.jseaes.2017.11.007.

Pu, G., Quackenbush, L.J., Stehman, S.V., 2021. Using google earth engine to assess temporal and spatial changes in river geomorphology and riparian vegetation. Journal of the American Water Resources Association 57 (5), 789-806. https://doi.org/10.1111/1752-1688.12950.

Putera, R., Junaidi, J., Junaidi, A., 2019. Analysis of Land Cover Changing and Vegetation Index at Kuranji Watershed in Padang, West Sumatera, Indonesia. Journal of Geoscience, Engineering, Environment and Technology 4 (4), 286-290.

Rahman, M.S., Di, L., Yu, E., Lin, L., Yu, Z., 2021. Remote Sensing Based Rapid Assessment of Flood Crop Damage Using Novel Disaster Vegetation Damage Index (DVDI). International Journal of Disaster Risk Science 12 (1), 90-110.

Setyorini, A., Khare, D., Pingale, S. M., 2017. Simulating the impact of land use/land cover change and climate variability on watershed hydrology in the upper brantas basin, Indonesia. Applied Geomatics 9 (3), 191-204. https://doi.org/10.1007/s12518-017-0193-z.

Slagter, B., Tsendbazar, N.E., Vollrath, A., Reiche, J., 2020. Mapping wetland characteristics using temporally dense Sentinel-1 and Sentinel-2 data: A case study in the St. Lucia wetlands, South Africa. International Journal of Applied Earth Observation and Geoinformation 86, 102009. https://doi.org/10.1016/j.jag.2019.102009.

Tarolli, P., Sofia, G., 2016. Human topographic signatures and derived geomorphic processes across landscapes. Geomorphology 255, 140-161.

https://doi.org/10.1016/j.geomorph.2015.12.007.

Obermann, A., Karyono, K., Diehl, T., Lupi, M., Mazzini, A., 2018. Seismicity at lusi and the adjacent volcanic complex, java, indonesia. Marine and Petroleum Geology 90, 149-156. https://doi.org/10.1016/j.marpetgeo.2017.07.033.

Orynbaikyzy, A., Gessner, U., Conrad, C., 2019. Crop type classification using a combination of optical and radar remote sensing data: A review. International Journal of Remote Sensing 40 (17), 6553-6595. https://doi.org/10.1080/01431161.2019.1569791.

Puigdefábregas, J., 2005. The role of vegetation patterns in structuring runoff and sediment fluxes in drylands. Earth Surface Processes and Landforms 30 (2), 133-147. https://doi.org/10.1002/esp.1181.

Urgeghe, A.M., Mayor, Á.G., Turrión, D., Rodríguez, F., Bautista, S., 2021. Disentangling the independent effects of vegetation cover and pattern on runoff and sediment yield in dryland systems – uncovering processes through mimicked plant patches. Journal of Arid Environments 193, 104585 (1-8). https://doi.org/10.1016/j.jaridenv.2021.104585.

Wang, S., Di Tommaso, S., Faulkner, J., Friedel, T., Kennepohl, A., Strey, R., Lobell, D.B., 2020. Mapping crop types in southeast India with smartphone crowdsourcing and deep learning. Remote Sensing 12 (18), 2957.

Wardlow, B.D., Egbert, S.L., 2010. A comparison of MODIS 250-m EVI and NDVI data for crop mapping: a case study for southwest Kansas. International Journal of Remote Sensing 31 (3), 805-830. https://doi.org/10.1080/01431160902897858.

Zulfakriza, Z., Saygin, E., Cummins, P.R., Widiyantoro, S., Nugraha, A.D., Lühr, B., Bodin, T., 2014. Upper crustal structure of central java, indonesia, from transdimensional seismic ambient noise tomography. Geophysical Journal International 197 (1), 630-635. https://doi.org/10.1093/gji/ggu016.

Zwaan, F., Corti, G., Sani, F., Keir, D., Muluneh, A.A., Illsley-Kemp, F., Papini, M., 2020. Structural analysis of the western afar margin, east africa: Evidence for multiphase rotational rifting. Tectonics 39 (7). e2019TC006043 (1-25). https://doi.org/10.1029/2019TC006043.